Activity of One of Two Engineered Heterodimers of AhpF, the NADH:Peroxiredoxin Oxidoreductase from *Salmonella typhimurium*, Reveals Intrasubunit Electron Transfer between Domains†

C. Michael Reynolds and Leslie B. Poole*

Department of Biochemistry, Wake Forest University School of Medicine, Winston-Salem, North Carolina 27157

Received December 5, 2000; Revised Manuscript Received January 23, 2001

ABSTRACT: AhpF, the flavoprotein reductase component of the *Salmonella typhimurium* alkyl hydroperoxide reductase system, catalyzes the reduction of an intersubunit disulfide bond in the peroxidatic active site of the system's other component, AhpC, a member of the peroxiredoxin family. Previous studies have shown that AhpF can be dissected into two functional units, a thioredoxin reductase-like C-terminus (containing FAD and a redox-active disulfide, Cys345−Cys348) and an N-terminal domain containing a second redox-active disulfide center (Cys129−Cys132). The role of the N-terminal domain as the direct reductant of AhpC, mediating electron transfer from the C-terminal redox centers of AhpF, has been firmly established by several approaches. Not known, however, was whether the transfer of electrons between the C-terminal and N-terminal disulfide centers occurred as an inter- or intrasubunit process in dimeric AhpF. Two heterodimeric AhpF species were therefore created in which one of the two pathways was completely disrupted while the other was left partially intact in each construct. Only the heterodimer containing one monomer of wild type AhpF and a monomer of mutated (and truncated) AhpF exhibited peroxidase activity with AhpC indicating that electron transfer between domains of AhpF is an intrasubunit process.

The alkyl hydroperoxide reductase system from *Salmonella typhimurium* consists of two proteins, AhpF and AhpC. Through reduction of organic hydroperoxides and hydrogen peroxide, these two proteins play a critical role in the cell's defense against oxidative damage (*1*, *2*). AhpF is a 57 kDa dimeric flavoprotein that utilizes reducing equivalents from NADH to reduce AhpC, a member of the peroxiredoxin family. AhpF is related to *Escherichia coli* thioredoxin reductase (TrxR);[1] residues 208−521 of AhpF are ∼35% identical to full-length TrxR (*3*, *4*). Like TrxR, the C-terminus of AhpF contains tightly bound flavin and a redox-active disulfide center (Cys345−Cys348). The N-terminus of AhpF, which is comprised of tandem repeats of two thioredoxin-like folds, contains a second redox-active disulfide center (Cys129−Cys132) required for catalysis of AhpC reduction (*5*, *6*). Paralleling the electron transfers in TrxR, the C-terminal portion of AhpF undergoes electron transfer from NADH to the Cys345−Cys348 redox center via the flavin. The Cys129−Cys132 redox center within AhpF's unique N-terminal domain then mediates the transfer of electrons from the dithiol form of the Cys345−Cys348 redox center to the intersubunit disulfide bond in the active site of AhpC.

Each molecule of AhpF is composed of two subunits in an antiparallel orientation (*7*), the same orientation observed in the crystal structure of TrxR (*8*). This head-to-tail arrangement, and the attachment of the N-terminal domain to the "far" end of the flavin domain of AhpF, suggested closer proximity of the Cys129−Cys132 redox center in the N-terminal domain to the redox-active disulfide center, Cys345′−Cys348′, in the pyridine nucleotide binding domain of the other subunit (*6*). Thus, the transfer of electrons from the C-terminal disulfide center to the N-terminal disulfide center of AhpF could occur between subunits of the AhpF dimer (Figure 1A, left side) (*5*, *6*). The alternative, that the N-terminal domain of AhpF interacts with the pyridine nucleotide binding domain in the same subunit, was also a consideration (Figure 1A, right side) (*9*). Previous studies demonstrated the presence of tryptic sensitive sites within the N-terminus up to residue 203, while the C-terminal fragment could be isolated intact by gel filtration chromatography (*10*). Thus, a long and presumably flexible linker between the N-terminal and C-terminal regions could bring the N-terminus into juxtaposition with the C-terminal disulfide center of the same subunit of AhpF for electron transfer interaction between disulfide centers (*9*). Flexibility in the

† This research was supported by National Institutes of Health Grant RO1 GM-50389 to L.B.P.

* To whom correspondence should be addressed: Department of Biochemistry, Wake Forest University School of Medicine, Medical Center Blvd., Winston-Salem, NC 27157. Phone: (336) 716-6711. Fax: (336) 716-7671. E-mail: lbpoole@wfubmc.edu.

[1] Abbreviations: TrxR, thioredoxin reductase; Trx, thioredoxin; F[1−202], truncated AhpF, including residues 1−202; F[208−521], truncated AhpF lacking residues 2−207; HET 1, heterodimer consisting of one subunit of F[208−521] and one subunit of AhpF^{C345,348S}; HET 2, heterodimer consisting of one subunit of F[208−521]^{C345,348S} and one subunit of wild type AhpF; DTNB, 5,5′-dithiobis(2-nitrobenzoate); TNB, 2-nitro-5-thiobenzoate; DMSO, dimethyl sulfoxide; FPLC, fast protein liquid chromatography; EDTA, ethylenediaminetetraacetic acid; LB, Luria-Bertani; SDS−PAGE, sodium dodecyl sulfate−polyacrylamide gel electrophoresis; AcPyAD$^+$, oxidized 3-acetylpyridine adenine dinucleotide; AcPyADH, reduced 3-acetylpyridine adenine dinucleotide; bp, base pairs; kb, kilobase pairs.

10.1021/bi002766h CCC: $20.00
Published on Web 03/09/2001

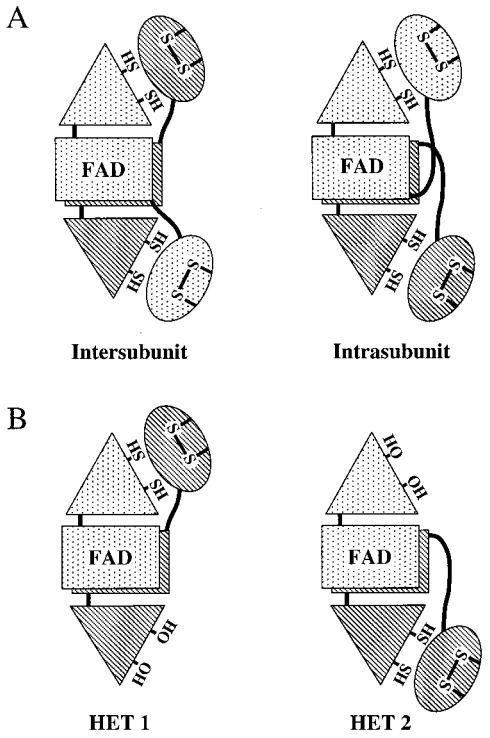

FIGURE 1: Potential pathways of electron transfer through dimeric AhpF (A) and heterodimeric AhpF constructs designed to elucidate the pathway (B). The two subunits of each dimer are depicted in a head-to-tail arrangement (2-fold axis of symmetry is horizontal and in the plane of the page) with different shading for each monomer. Shown as different shapes are the flavin-binding (rectangles), pyridine nucleotide binding (triangles), and N-terminal (ellipses) domains of AhpF. Redox-active disulfide centers are depicted as reduced, $(SH)_2$, in the pyridine nucleotide binding domain and oxidized (S−S) in the N-terminal domain, as they would be prior to electron transfer between them. Sites of cysteine replacement with serine residues are shown as $(OH)_2$. In panel A, the intersubunit pathway of electron transfer (left) depicts the Cys345−Cys348 dithiol form in one subunit reducing the oxidized Cys129−Cys132 center in the other subunit. The intrasubunit pathway of electron transfer (right) shows the Cys345−Cys348 dithiol form of one subunit reducing the oxidized Cys129−Cys132 center of the same subunit. In panel B, HET 1 (left) consists of one subunit of F[208−521] and one subunit of $AhpF^{C345,348S}$ and would be active as an AhpC reductase only if the intersubunit pathway of electron transfer is operable. Likewise, HET 2 (right) consists of one subunit of $F[208-521]^{C345,348S}$ and one subunit of wild type AhpF and is competent to transfer electrons only through the intrasubunit pathway.

linker could also be important for large domain movements hypothesized to occur during catalysis between multiple redox centers (*9*, *11*).

Recent X-ray crystallographic data have provided our first glimpse of some of the structural attributes of AhpF, yet the question of inter- versus intrasubunit transfer was not initially resolved by that information (*9*). Indeed, distances between N-terminal and C-terminal redox centers, ∼35 and ∼33 Å for inter- and intrasubunit pathways, respectively, are prohibitive in either case without significant domain movement. We therefore set out to establish the pathway of electron transfer among the redox centers within dimeric AhpF. Described herein are experiments whereby catalytic activities of two different heterodimeric AhpF species were measured. In each construct, one of the two possible electron transfer pathways has been completely disrupted, while the alternative pathway is retained in half of the dimeric molecule (Figure 1B). We have now clearly established that only the intrasubunit pathway of electron transfer between domains is operable in AhpF during catalysis with AhpC; only one of the two constructs (HET 2) exhibits substantial disulfide-reducing activity.

EXPERIMENTAL PROCEDURES

Materials. NADH was purchased from Boehringer Mannheim. Sigma was the supplier of L-(+)-arabinose, α-lactose, FAD, 3-acetylpyridine adenine dinucleotide ($AcPyAD^+$), streptomycin sulfate, cumene hydroperoxide (80%), and molecular biology grade ammonium sulfate. Other reagents and buffer components, including 5,5′-dithiobis(2-nitrobenzoate) (DTNB), glycerol, dimethyl sulfoxide (DMSO), and sodium dodecyl sulfate (SDS), were purchased from Research Organics, Inc. Difco bacteriological media and organic solvents were from Fisher. Acrylamide (40%) was purchased from Bio-Rad. Restriction enzymes and DNA-modifying enzymes were obtained from Promega and New England Biolabs.

Construction of Compatible Expression Plasmids. In creating heterodimeric AhpF proteins containing either $AhpF^{C345,348S}$ and F[208−521] (the C-terminal fragment lacking the first 207 residues) or wild type AhpF and $F[208-521]^{C345,348S}$, designated HET 1 and HET 2, respectively (Figure 1B), we tried several approaches. Subunit exchange to promote heterodimer formation on mixing purified homodimers was not effective according to pilot studies employing this technique. Coexpression of two proteins from a single pAF1-derived plasmid (*2*), with protein expression under control of the T7 promoter, gave very low levels of the first of two open reading frames, even when sequences upstream of the ATG initiation codons were identical (data not shown). Ultimately, success was obtained by expressing the full-length protein of each pair from an arabinose-inducible pBAD plasmid (*12*) and the truncated protein partner from pAF[208−521], a derivative of pAF1 (Figure 2). To generate HET 1 (Figure 1B, left side), $p_{BAD}F^{C345,348S}$ was created and used for coexpression with pAF[208−521] described previously (*6*). Briefly, a 1.8 kb *Kpn*I−*Pst*I restriction fragment encoding the C345,348S mutant of AhpF in a pBluescriptII SK(+) (Stratagene, La Jolla, CA) derivative, pBlF2 (*5*), was isolated and ligated into the corresponding sites of p*Trc*99A (Amersham Pharmacia Biotech Inc., Piscataway, NJ) using standard DNA manipulation techniques (*13*). Subsequent transfer of a 1.8 kb *Kpn*I−*Hin*dIII fragment from the p*Trc*99A-derived plasmid to the corresponding sites in pBAD30 generated $p_{BAD}F^{C345,348S}$ (Figure 2A). In all cases, newly generated expression plasmids were sequenced through the entire coding region to ensure the lack of additional inadvertent mutations (DNA sequence analyses were conducted by the core facility of the Comprehensive Cancer Center of Wake Forest University).

The production of HET 2 (Figure 1B, right side) was accomplished through coexpression of the full-length wild type with truncated, mutant AhpF from $p_{BAD}F$ and $pAF[208-521]^{C345,348S}$, respectively (Figure 2B). $p_{BAD}F$ was generated as described above for $p_{BAD}F^{C345,348S}$ except that wild type pBlF2, rather than the mutant, was used as the source of the initial *Kpn*I−*Pst*I fragment. $pAF[208-521]^{C345,348S}$ was created through subcloning of a 713 bp *Eag*I−*Bst*XI fragment

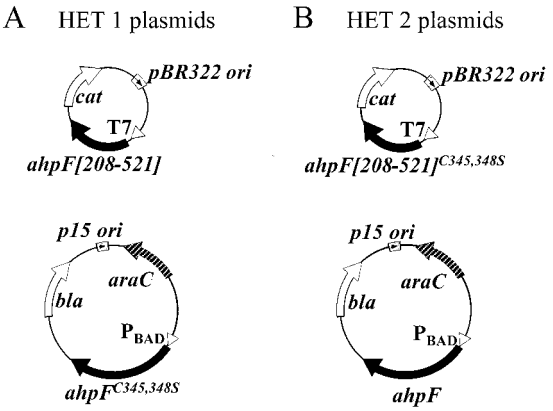

FIGURE 2: Compatible expression plasmids used to generate HET 1 (A) or HET 2 (B). Either pAF[208−521] (A, top) or a pAF-[208−521] derivative expressing a mutated (C345,348S), truncated AhpF protein (B, top) was transformed into the JM109(DE3) strain of *E. coli* already harboring either $p_{BAD}F^{C345,348S}$ (A, bottom) or $p_{BAD}F$ (B, bottom) to create HET 1 or HET 2, respectively. Construction of these plasmids is described in Experimental Procedures. In each case, the pAF1 (top, 3588 bp) and pBAD30 (bottom, 6671 bp) derived plasmids were comaintained in the host bacterium through their different origins of replication (derived from pBR322 or p15, respectively) and continual selection for both antibiotic resistance phenotypes with chloramphenicol and ampicillin. Protein expression is also under the control of different promoters [T7 RNA polymerase-dependent (T7) or arabinose-dependent (P_{BAD})] in these constructs.

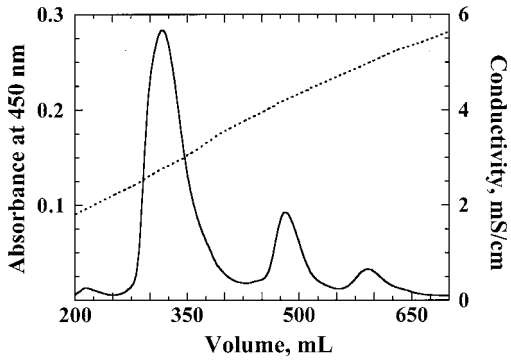

FIGURE 3: Elution profile demonstrating separation of homodimers from HET 2 using Q Sepharose chromatography. Dialyzed crude extracts from a pAF[208−521]^{C345,348S}- and p_{BAD}F-harboring JM109-(DE3) *E. coli* strain (plasmids shown in Figure 2B) were prepared as described in Experimental Procedures and applied to a 70 mL Q Sepharose Fast Flow (FPLC) column preequilibrated in 5 mM potassium phosphate at pH 7.0 containing 0.2 mM EDTA. Following a 350 mL wash with the same buffer, proteins were eluted with a linear gradient from 5 to 80 mM potassium phosphate buffer (900 mL total). Shown are the three prominent peaks which corresponded to the F[208−521]^{C345,348S} homodimer, the HET 2 heterodimer, and the AhpF homodimer (in order of elution), with A_{450} plotted as a function of the gradient volume. The dotted line represents the conductivity measured over the course of the gradient (right axis). Fractions were collected in volumes of 9.6 mL each (not shown). The corresponding profile for HET 1 purification was essentially identical.

from the C345,348S-expressing mutant of pAF1 (*5*) into pAF[208−521]. Each pair of plasmids was transformed (one at a time) into competent JM109(DE3) cells by the TSS method (*14*). In each case, both plasmids were stably maintained on Luria-Bertani (LB) broth plates and in liquid cultures where both ampicillin (50 μg/mL) and chloramphenicol (25 μg/mL) were included.

Purification Procedures for Generating HET 1 and HET 2. Single colonies of JM109(DE3) harboring either $p_{BAD}F^{C345,348S}$ and pAF[208−521] or p_{BAD}F and pAF[208−521]^{C345,348S} were subcultured in 4 and 100 mL of LB broth containing ampicillin and chloramphenicol. The latter culture was then used to inoculate 10 L of LB medium in a New Brunswick BioFlo 2000 fermentor containing the same antibiotics as well as 0.2% (w/v) L-(+)-arabinose, 0.5% (w/v) α-lactose, 0.35% (w/v) monobasic potassium phosphate, and 0.5% (w/v) dibasic potassium phosphate. Cultures were agitated, sparged with filtered air, and maintained at 37 °C. When an A_{600} of ∼4.5 was reached, arabinose and lactose were once again added to the culture to achieve final concentrations of 4 and 1%, respectively, and the growth was continued for an additional 12 h before the cells were harvested by centrifugation. Cell pellets were stored at −20 °C until they were needed.

A single protocol was used for the purification of both heterodimeric proteins. A standard buffer of 25 mM potassium phosphate (pH 7.0) containing 1 mM EDTA was used unless otherwise indicated. Streptomycin sulfate-treated cell extracts from mechanical cell disruption with glass beads were brought to 30% ammonium sulfate in the standard buffer, centrifuged to remove the pellet, and then brought to 75% ammonium sulfate for collection of the precipitated proteins essentially as described previously (*2*). The resuspended pellet was dialyzed extensively against 5 mM potassium phosphate (pH 7.0) containing 0.2 mM EDTA before loading on a 70 mL Q Sepharose Fast Flow column preequilibrated with the same buffer. This chromatographic step was carried out using an Äkta Explorer 10S FPLC instrument (Amersham Pharmacia Biotech Inc.). The column was washed with the 5 mM potassium phosphate buffer and then eluted with a linear gradient from 5 to 80 mM potassium phosphate. Three flavin-containing peaks were detected by monitoring 450 nm absorbance during the elution of the Q Sepharose column (Figure 3). As expected, the first and largest peak contained the homodimeric truncated protein; F[208−521] had previously been shown to elute at lower ionic strength than intact AhpF from a comparable anion-exchange column (*6*). The third and smallest peak eluted at an ionic strength at which full-length AhpF had previously been shown to elute from a similar Q Sepharose column. The intermediate peak contained the putative heterodimeric AhpF species (as verified by nondenaturing polyacrylamide gels described below). Fractions from the center of the second peak were pooled and immediately loaded on a 100 mL Affi-Gel Blue (Bio-Rad) column that had been pre-equilibrated in the standard buffer. The column was washed and then eluted with a 700 mL linear gradient from the standard buffer to 0.6 M potassium phosphate (pH 7.0) containing 0.3 M NaCl and 1 mM EDTA. Fractions were analyzed on both nondenaturing and denaturing polyacrylamide gels such as those shown in Figure 4 (*15*). Those containing the pure heterodimer were pooled and concentrated by ultrafiltration in an 8000 Series stirred cell from Millipore (Bedford, MA) using a YM30 membrane. Redilution and concentration of each protein by ultrafiltration resulted in an exchange of buffers to one containing 0.6 M potassium phosphate, 0.3 M NaCl, 1 mM EDTA, and 20% (v/v) glycerol at pH 7.0. Storage of each protein in this buffer at −80 °C led to essentially no dissociation of heterodimers over at least 5 months, whereas low levels of heterogeneity

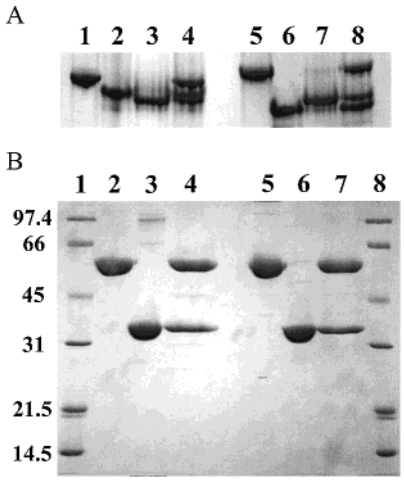

FIGURE 4: (A) Native and (B) SDS−polyacrylamide gel electrophoresis of HET 1, HET 2, and the respective homodimeric parent proteins. Samples analyzed on the native polyacrylamide gel shown in panel A were as follows: lanes 1 and 5, the full-length homodimers, AhpF^{C345,348S} and wild type AhpF, respectively; lanes 2 and 6, the truncated homodimers, F[208−521] and F[208−521]^{C345,348S}, respectively; and lanes 3 and 7, the purified heterodimers, HET 1 and HET 2, respectively. Lane 4 contained the same three proteins analyzed in lanes 1−3, and lane 8 contained all three proteins analyzed in lanes 5−7. Lanes 1−3 and 5−7 contained 12 μg of each protein; lanes 4 and 8 contained 6 μg of each protein. Samples analyzed on the denaturing polyacrylamide gel in panel B were pretreated by heating at 85 °C for 3 min in sample buffer containing SDS and 2-mercaptoethanol. Lanes 2 and 5 contained the full-length homodimers, AhpF^{C345,348S} and wild type AhpF, respectively; lanes 3 and 6 contained the truncated homodimers, F[208−521] and F[208−521]^{C345,348S}, respectively, and lanes 4 and 7 contained the heterodimers, HET 1 and HET 2, respectively. All lanes contained 12 μg of the respective proteins. Lanes 1 and 8 contained low-range protein standards from Bio-Rad with the indicated M_r values.

developed over time (as observed on nondenaturing gels) when heterodimeric proteins were stored at −20 °C in standard buffer.

Other Protein Purification Procedures. F[208−521]^{C345,348S} was purified from fractions within the first peak that eluted from the Q Sepharose column during the purification of the F[208−521]^{C345,348S}/wild type AhpF heterodimer (HET 2) described above. Fractions containing homodimeric F[208−521]^{C345,348S} were pooled and rechromatographed on Affi-Gel Blue as described for the heterodimeric proteins. The pure protein, as determined by SDS−PAGE, was pooled, dialyzed against the standard buffer, and stored at −20 °C until further use. *S. typhimurium* wild type AhpF and AhpC proteins were expressed and purified as previously described (*2*). Purification procedures for isolating F[208−521] and AhpF^{C345,348S} were also described previously (*5*, *6*).

Polyacrylamide Gel and Densitometric Methods. Nondenaturing (7.5%) and SDS-containing (10%) polyacrylamide gels were prepared as described previously (*15*). Protein samples prepared in buffer without SDS or 2-mercaptoethanol were electrophoresed at 30 mA for 3 h for native gels, while 2% SDS- and 5% 2-mercaptoethanol-containing samples were heated at 85 °C for 3 min and electrophoresed at 45 mA in the presence of 1% SDS until the blue dye reached the bottom for denaturing gels (∼1.5 h). The presence of SDS in samples and buffers used with the denaturing gel, but not with the native gel, and the presence of 2-mercaptoethanol in samples applied to the denaturing gel were the only major differences between the two procedures. Protein gels were soaked in water for three 5 min changes and stained with Gelcode Blue stain reagent from Pierce (Rockford, IL). Densitometry to assess the protein contents of bands within the HET 2 samples analyzed on native gels was carried out using Version 4 of the Quantity One Quantitation Software from Bio-Rad Laboratories (Hercules, CA) and the image files generated with an AlphaImager 2200 Gel Documentation and Analysis System from Alpha Innotech Corp. (San Leandro, CA). Image files were generated using a visible light source, an aperture setting of 1/22, and 1/30 s exposures. For quantitation, six amounts of wild type AhpF (0.5−2.5 μg) were electrophoresed along with varying amounts of HET 2 on the same gel. A standard curve (correlation coefficient > 0.99) was then generated from the AhpF data and used to determine the amount of protein in individual bands of HET 2 which were within the linear range of this method. On the basis of this technique, it was possible to conclude that the amount of contaminating wild type AhpF homodimer in the HET 2 pool was less than 5% of the total protein.

Spectroscopic Experiments. Either a Milton Roy Spectronic 3000 diode array spectrophotometer with 0.35 nm resolution or an Applied Photophysics DX.17MV stopped-flow spectrofluorometer, thermostated at 25 °C, was used to conduct enzymatic assays. A Beckman DU 7500 spectrophotometer equipped with microcuvettes was used in the determination of the extinction coefficient of the bound flavin of each heterodimer. The molar extinction coefficients of the protein-bound FAD at 450 nm were determined by release of the flavin cofactor with 4 M guanidine hydrochloride and quantitation of the corresponding free FAD (*10*). The extinction coefficients for the homodimeric proteins were determined in standard buffer, while the extinction coefficients for the bound FAD of HET 1 and HET 2 were determined in the 25 mM phosphate buffer as well as the high-salt/glycerol buffer in which the proteins were stored. Extinction coefficients used for all reduced and oxidized pyridine nucleotides, free FAD, and TNB were those previously reported (*2*).

Analytical Ultracentrifugation Studies. Sedimentation equilibrium analyses were performed essentially as described previously (*6*). Heterodimeric proteins were washed in Centricon CM-50 ultrafiltration assemblies immediately prior to sedimentation equilibrium analyses to exchange the high-salt/glycerol storage buffer for standard buffer containing 150 mM NaCl. Four concentrations each (115 μL per sample) of HET 1 and HET 2, from 3 to 34 μM, were loaded into six-sectored Epon charcoal centerpieces from Beckman Instruments Inc. (Palo Alto, CA) along with 125 μL into reference sectors of the buffer from the final filtrate following ultrafiltration. Data for samples at 20 °C after 8, 10, and 12 h at each speed were acquired using a Beckman Optima XL-A analytical ultracentrifuge and an interfaced Toshiba Equium 7100D computer running Windows 95. Global analysis of multiple data sets (both 280 and 450 nm data) obtained at 8000, 9500, and 14 000 rpm was performed using the Windows version of NONLIN (*16*). No data at or above 1.4 absorbance units were used in the analyses. A value of 0.7430 cm^3 g^{-1} was calculated for the partial specific volume of both heterodimers from their amino acid compositions (*17*). The solvent density, at 1.0058 g cm^{-3}, was measured

Table 1: Catalytic Activities of Homodimeric and Heterodimeric AhpF Proteins[a]

activity	AhpF^{C345,348S}	F[208−521]	HET 1	AhpF	F[208−521]^{C345,348S}	HET 2
transhydrogenase[b]	2000 ± 260	1810 ± 350	1820 ± 170	1820 ± 210	2940 ± 790	1850 ± 150
DTNB reductase[c]	<10	38.1 ± 1.0	16.7 ± 1.1	1490 ± 40	<10	644 ± 27
peroxidase[d]						
k_{cat}[e]	<1	<1	<1	13100 ± 400	<1	5330 ± 160
K_m^{AhpC}[f]	NA[g]	NA	NA	14.0 ± 1.3	NA	49.6 ± 3.0

[a] Values reported as means ± standard error. [b] Transhydrogenase activity was measured aerobically in assay buffer 1 [50 mM Tris-HCl (pH 8.0), 0.5 mM EDTA, and 100 mM ammonium sulfate] with 150 μM NADH and 150 μM AcPyAD$^+$ in a total volume of 1.0 mL at 25 °C; values are expressed as micromoles of AcPyADH formed per minute per micromole of bound FAD. [c] DTNB reductase activity was measured aerobically in assay buffer 1 (above) with 50 μM NADH and 500 μM DTNB, in a total volume of 1.0 mL at 25 °C; values are expressed as micromoles of DTNB reduced per minute per micromole of bound FAD. [d] Peroxidase activity was measured aerobically in assay buffer 2 [50 mM potassium phosphate (pH 7.0), 0.5 mM EDTA, and 100 mM ammonium sulfate] with 1 mM cumene hydroperoxide and 150 μM NADH at 25 °C; rates were adjusted for the very low rate of NADH consumption by the flavoprotein in the absence of AhpC. [e] Values are expressed as micromoles of NADH oxidized per minute per micromole of bound FAD. [f] K_m^{AhpC} expressed in micromolar. [g] NA, not applicable.

using a DA-310M precision density meter (Mettler Toledo, Highstown, NJ) thermostated at 20 °C.

Activity Assays. Purified HET 1 and HET 2 proteins were maintained on ice in the high-salt/glycerol buffer until their final dilutions into the respective assay mixtures. Standard assays for transhydrogenase and DTNB reductase activities were carried out as previously described (*2*) in buffers containing 100 mM ammonium sulfate. Protein concentrations used in the DTNB reductase assays ranged from 1−10 nM for wild type AhpF and HET 2 to 40−160 nM for the other proteins (Table 1). Steady-state peroxidase assays with AhpC were carried out on the stopped-flow spectrofluorometer (using the linear data collected between 0.5 and 2 s) with 0.2 μM HET 2 or 0.1 μM AhpF in the presence of 150 μM NADH, 1 mM cumene hydroperoxide, 50 mM potassium phosphate at pH 7.0, 0.5 mM EDTA, and 100 mM ammonium sulfate. Assays with AhpF employed 3.5−56 μM AhpC, while assays with HET 2 required a greater range of AhpC concentrations, from 3.5 to 150 μM, to determine k_{cat} and K_m values. Kinetic parameters were calculated from the data using the program ENZFITTER (*18*). Due to the lack of AhpC-linked peroxidase activity for F[208−521], F[208−521]^{C345,348S}, AhpF^{C345,348S}, and HET 1, complete sets of steady-state assays were not carried out with these proteins. Each of these proteins, at 2.5 μM, was assayed with 20 μM AhpC and found to have minimal activity.

RESULTS

Purification and Characterization of Two Heterodimers of AhpF, HET 1, and HET 2. To address the issue of inter- versus intrasubunit electron transfer between C-terminal and N-terminal disulfide centers of AhpF, heterodimers of mutant and wild type proteins were designed such that only one of the two pathways would be available to each heterodimer (Figure 1). Truncation constructs with the N-terminus completely removed, rather than constructs with the more conservative mutation of the N-terminal active site cysteines to serine residues (C129,132S), were chosen for coexpression with full-length constructs to alter the chromatographic properties of the heterodimers and facilitate their purification (Figure 2). In designing these experiments, we relied on information from our earlier characterization of fragments of AhpF (F[1−202] and F[208−521]) which indicated that these regions of AhpF fold independently and share considerable structural and functional properties with intact AhpF (*6*). These previous studies also established that the dimer interface within AhpF lies largely or wholly within the C-terminal part of the molecule, making feasible the creation of the proposed heterodimers.

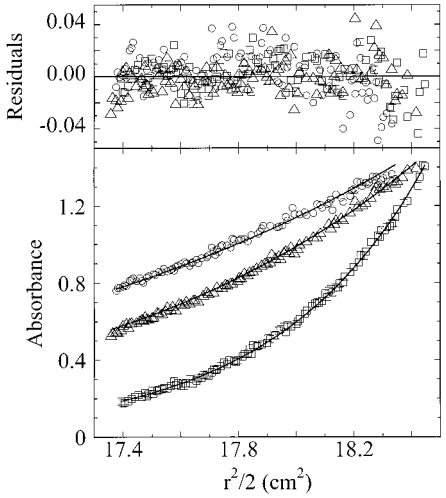

FIGURE 5: Sedimentation equilibrium analyses of HET 2 to determine molecular weights. Shown are single data sets recorded at 280 nm for 88 μM HET 2 equilibrated at 20 °C and 8000 (○), 9500 (△), and 14 000 rpm (□). Solid lines represent global fits to a single ideal species model of 14 data sets at 280 and 450 nm, four concentrations, and all three rotor speeds. The top panel depicts the deviations between the experimental and calculated data (residuals) for each data set.

On coexpression of full-length and truncated AhpF proteins, heterodimeric species, designated HET 1 and HET 2, were generated and isolated from homodimeric "parent" proteins by anion-exchange chromatography (Figure 3). Although the expression of the full-length and truncated proteins was not balanced due to the higher copy number and stronger promoter of the plasmids bearing the truncated constructs, there was sufficient production of the full-length proteins to result in a reasonable yield of each heterodimer (12−15 mg of pure protein from 10 L of bacterial growth medium). Following an additional purification step (affinity chromatography with Affi-Gel Blue), isolated heterodimers were stored at −80 °C in a high-salt buffer with glycerol to prevent subunit exchange.

The heterodimeric nature of the isolated proteins was confirmed by their characteristic patterns on nondenaturing and denaturing polyacrylamide gels (Figure 4) and by analytical ultracentrifugation studies (Figure 5). Each heterodimer, HET 1 (F[208−521]/AhpF^{C345,348S}) and HET 2

(F[208−521]^{C345,348S}/AhpF), migrates to a position on native gels that is distinguishable from those of either of its respective homodimeric "parent" proteins (Figure 4A). On the other hand, each purified heterodimeric protein yields approximately equal molar amounts of full-length (55 kDa) and truncated (36 kDa) AhpF when electrophoresed under reducing and denaturing conditions (Figure 4B). Data from sedimentation equilibrium analyses were also consistent with heterodimeric full-length and truncated proteins in each case. Global fits of the data to a single ideal species model using multiple concentrations of proteins analyzed at different rotor speeds (Figure 5) gave weight-average molecular weight (M_w) values of 85 100 ± 2600 and 86 200 ± 2300 for HET 1 and HET 2, respectively (the theoretical M_w of each heterodimer is 89 283). Analyses using more complex models taking into account the possible equilibrium between monomers and dimers did not improve the fits and were not statistically justified.

Comparisons of Spectroscopic Properties of HET 1, HET 2, and the Homodimeric Parent Proteins. F[208−521], one component of HET 1, was previously reported to exhibit a visible spectrum which was virtually indistinguishable from that of wild type AhpF (*6*). Likewise, F[208−521]^{C345,348S} (a HET 2 component) exhibits a visible spectrum nearly identical to the spectrum of AhpF^{C345,348S}, a mutant exhibiting only minor perturbations in absorbance properties relative to those of wild type AhpF (λ_{max} for the first of the two flavin peaks is slightly blue-shifted, at 377 nm instead of 381 nm for the wild type, and the extinction coefficient at 450 nm is slightly lower) (*5*). HET 1 and HET 2 exhibit ultraviolet and visible spectra with properties intermediate between those of the spectra of the homodimeric parent proteins. The extinction coefficients at 450 nm for AhpF (13 100 M^{-1} cm^{-1}) (*2*), AhpF^{C345,348S} (11 800 M^{-1} cm^{-1}) (*5*), and F[208−521] (12 900 M^{-1} cm^{-1}) (*6*) have been reported previously. F[208−521]^{C345,348S}, with one FAD bound per subunit, has an extinction coefficient of 12 100 M^{-1} cm^{-1} at 450 nm. Extinction coefficients at 450 nm for HET 1 are 12 300 and 12 600 M^{-1} cm^{-1} in the high-salt/glycerol storage buffer and standard phosphate buffer, respectively. HET 2 has an extinction coefficient of 12 200 M^{-1} cm^{-1} in both buffers. Ratios of absorbance values at 280 and 450 nm were intermediate (4.9 and 5.0, respectively) for HET 1 and HET 2 compared with those observed for full-length [5.4 for AhpF (*2*) and 5.2 for AhpF^{C345,348S}] and truncated [4.7 for F[208−521] (*6*) and 4.5 for F[208−521]^{C345,348S}] proteins.

Flavin-Mediated Transhydrogenase Activities of HET 1, HET 2, and Homodimeric AhpF Proteins. Transhydrogenase activity assays, which assess hydride transfer from NADH to an oxidized pyridine nucleotide analogue of higher potential ($AcPyAD^+$) mediated by the enzyme's bound flavin, are useful in comparing mutant or truncated proteins as a functional assessment of their proper folding and flavin binding properties. Previous studies have shown that both redox-active disulfide-mutated and N-terminally truncated AhpF proteins retain this activity (*5*, *6*). Our results, summarized in Table 1, confirm that the homodimeric parent proteins retain transhydrogenase activity and reveal that both HET 1 and HET 2 exhibit high transhydrogenase activity as well. These heterodimeric proteins are therefore fully functional by one measure of flavin-mediated enzymatic activity.

NADH-Dependent DTNB and AhpC-Linked Peroxide Reductase Activities of HET 1, HET 2, and Related Homodimeric AhpF Proteins. Functional assays whereby the bound flavin and the two disulfide centers of AhpF mediate electron transfer between NADH and AhpC, and subsequently to cumene hydroperoxide, have been described previously (*2*). This enzymatic process can be monitored on the basis of the oxidation of NADH and the associated decrease in absorbance at 340 nm. Another substrate for AhpF, the disulfide-containing small molecule DTNB, is readily reduced by the intact flavoprotein and generates a chromophoric product, TNB, detected at 412 nm. Assays of mutant and truncated proteins have shown that alterations in AhpC-linked peroxidase activities are also associated with parallel effects on DTNB reductase activities, although a low level of the latter activity remains in several AhpF mutants lacking one or both redox-active disulfide centers (*5*, *6*). Both assays were therefore used to assess the nature of the pathway of electron transfer between C-terminal and N-terminal disulfide centers in AhpF.

As shown in Table 1, mutated and/or truncated homodimeric AhpF proteins exhibited only low DTNB reductase activities [<40 μmol of DTNB reduced min^{-1} (μmol of bound FAD)$^{-1}$] compared with that of wild type AhpF [∼1500 μmol of DTNB reduced min^{-1} (μmol of bound FAD)$^{-1}$]. Only one of the two heterodimeric proteins, HET 2, exhibits appreciable DTNB reductase activity. HET 2 exhibited 43% of the DTNB reductase activity of wild type AhpF, while HET 1 exhibited less than 2% of the activity observed with the wild type protein. As previously demonstrated, the K_m value of AhpF for DTNB, estimated to be in the low millimolar range, cannot be accurately assessed due to the high background absorbance at 412 nm for DTNB above ∼1.5 mM (*2*). Instead, the DTNB reductase activities of HET 2 and wild type AhpF were compared over a range of DTNB concentrations from 300 to 1200 μM. In all cases, HET 2 activity was 40−45% of that of wild type AhpF, suggesting that the K_m of HET 2 for DTNB is unchanged from that of the wild type protein.

Results of flavoprotein-dependent peroxidase assays carried out aerobically in the presence of saturating substrates (150 μM NADH and 1 mM cumene hydroperoxide) paralleled the results of the DTNB reductase assays as shown in Table 1. All mutant and/or truncated homodimeric proteins were devoid of significant AhpC-linked peroxidase activity. HET 2, on the other hand, had considerable activity, with a k_{cat} of 5330 min^{-1} (41% of the activity of wild type AhpF), while HET 1 did not exhibit detectable activity. The decrease in k_{cat} to about half of that of wild type AhpF was expected for the active heterodimer; only one-half the normal number of redox-active disulfide centers of wild type AhpF is present in either heterodimer. On the other hand, the >3-fold increase in the K_m value of HET 2 for AhpC, at about 50 μM compared with 14 μM for wild type AhpF, was a rather unexpected result. By comparison, the K_m for an alternative oxidizing substrate, DTNB, does not appear to be different for the two proteins (vide supra).

Several additional controls were carried out to establish the validity of our HET 2 data. First, wild type AhpF and F[208−521]^{C345,348S}, the "parents" of HET 2, were mixed in equimolar amounts and evaluated for AhpC-linked peroxidase activity. Values of 6600 min^{-1} for k_{cat} and 15 μM for

K_m^{AhpC} were obtained, corresponding to about half the k_{cat} value of AhpF and about the same K_m value as wild type AhpF. As described in Experimental Procedures, peroxidase assays were carried out using a stopped flow spectrophotometer, and activity measurements were complete within ~2 s of mixing. Nonetheless, to ensure that HET 2 subunits do not dissociate and reassociate extensively to produce homodimers under these conditions, samples of HET 2 were diluted into peroxidase assay buffer in the presence or absence of substrates for approximately 5 min followed by reconcentration using CM-50 ultrafiltration units and analysis on nondenaturing gels. Analyses of the bands by densitometry verified the stability of the HET 2 heterodimer under these conditions, as the intensity of the upper band representing the wild type AhpF homodimer was not increased in either of these cases. Taken together with the results described above, these findings demonstrate that HET 2 is an active heterodimer with unique kinetic parameters distinctly different from those of the wild type enzyme.

DISCUSSION

The isolation of heterodimeric proteins HET 1 (F[208−521]/AhpF^{C345,348S}) and HET 2 (F[208−521]^{C345,348S}/wild type AhpF) for elucidation of the pathway of electron transfer between redox centers in dimeric AhpF (Figure 1) was accomplished by the development of separate expression plasmids for each component (Figure 2). Furthermore, one of the two components of each heterodimer lacked 207 residues at the N-terminus, allowing for efficient purification of each heterodimer from contaminating homodimers by anion-exchange chromatography (Figure 3). Direct proof that HET 1 and HET 2 were indeed pure heterodimers was obtained by nondenaturing and denaturing polyacrylamide gel electrophoresis (Figure 4). Each heterodimer exhibited a unique electrophoretic mobility on nondenaturing gels when compared with the mobilities of the related homodimeric proteins, while SDS−PAGE demonstrated the presence of equimolar amounts of full-length and truncated proteins in these samples. Spectral characteristics and molecular weight values obtained by sedimentation equilibrium analyses (Figure 5) also fully supported the intermediate properties of these heterodimers relative to the homodimers. All species under investigation exhibited high transhydrogenase activities (Table 1) consistent with proper folding and flavin binding to these engineered proteins.

The fact that electron transfer between C-terminal and N-terminal disulfide centers is an intrasubunit process in AhpF was established by the substantial disulfide reductase activity exhibited by HET 2 (~42% compared with wild type AhpF), but not HET 1 (Table 1). As densitometric analyses indicated that the level of contamination of the HET 2 pool by wild type AhpF homodimer was less than 5%, and no change in homodimer content was observed on dilution of HET 2 into peroxidase assay buffer in the presence of substrates, the activity observed for HET 2 by both types of assays could not be a result of wild type AhpF homodimer contamination or generation during the assays. Only the intrasubunit pathway of electron transfer is operable in HET 2 through half the normal complement of redox-active disulfide centers, accounting for the partial activity observed in this construct (Figure 1). HET 1, where the intersubunit pathway of electron transfer is intact in half of the dimer, displayed essentially no reactivity toward DTNB or AhpC, eliminating this as a viable pathway for electron transfer through AhpF. Perturbations in AhpC-linked peroxidase activities resulting from mutations and truncations of AhpF have been shown to parallel those in DTNB reductase activities in previous experiments (*9*), and that pattern has been maintained in these studies as well. Thus, the DTNB-reducing activity of AhpF is also reliant on an intact N-terminal disulfide center and a similar mechanism for catalysis (relative to the physiological substrate AhpC). The fact that the N-terminal domain is essential for strong disulfide reductase activity with AhpC or DTNB was also clearly demonstrated by the appearance of these activities in a chimeric protein in which the 207 N-terminal amino acids from AhpF were fused to TrxR from *E. coli* (TrxR alone cannot reduce AhpC or DTNB) (*19*). On the basis of the results presented here, electron transfer between TrxR and N-terminal portions of the chimera is almost certainly a mandatory intrasubunit process, as well.

The increase in the K_m value for AhpC of HET 2 relative to that of wild type AhpF deserves special attention. In the heterodimer, a wild type AhpF monomer is bound to a truncated, inactive monomer rather than to another active AhpF monomer, and it is possible that AhpF−AhpC interactions could be perturbed by effects communicated across the dimer. It is difficult, however, to envision such "dimer interface" effects as having much impact on AhpF−AhpC interactions occurring at the N-terminal domain. As an alternative explanation, the K_m value of wild type AhpF for AhpC might reflect interactions that occur at two sites simultaneously for AhpF and AhpC dimers when the latter is at high concentrations. In HET 2, one of these two interactions per dimer would be lost, possibly leading to the higher K_m observed for this heterodimer in comparison with that of wild type AhpF. Testing of full-length heterodimeric proteins with or without mutations at the N-terminus could help to resolve the origin of this K_m effect in HET 2. A further implication of the higher K_m^{AhpC} value observed for HET 2 relative to that of wild type AhpF is that the former clearly represents a distinct form of AhpF and not homodimeric AhpF diluted with an inactive homodimer. Control experiments have established that the K_m^{AhpC} does not change in the latter case.

In very recent crystallographic analyses of AhpF (*7*) and comparisons with the recently reported "twisted" conformation of TrxR from *E. coli* (*20*), domain movements modeled for AhpF could account for intrasubunit, but not intersubunit, electron transfer between C-terminal and N-terminal disulfide centers. In this "twisted AhpF" model, Cys129 and Cys348 are in closest proximity for formation of a transient "intercenter" disulfide bond, and may represent the interacting residues during that catalytic step. Our biochemical studies and the independent structural analyses have therefore very nicely complemented one another and have both confirmed intrasubunit electron transfer within AhpF.

Our approach to expression and isolation of heterodimeric proteins to distinguish between intra- and intersubunit interactions in AhpF, although reliant on coexpression of components rather than subunit exchange between purified homodimers, was similar to that for the full-length and truncated heterodimers created for studies of the transsubunit interactions of tyrosyl tRNA synthetase with $tRNA^{Tyr}$ (*21*).

Other heterodimeric constructs have also been generated (and subsequently purified) through engineering to include epitope tags or polyhistidine and/or polyarginine residues on one of the two subunits of the dimer or by having different "tags" on each subunit of the dimer (*22*−*24*). The purity of heterodimers has not always been readily addressed by these methods, although in our case the unique mobilites of each heterodimer on nondenaturing polyacrylamide gels were clearly diagnostic.

Our studies have provided a clearer picture of how electron transfer to disulfide bonds in protein substrates can be accomplished when the initial transfer is between reduced pyridine nucleotide and bound flavin, and the site of substrate reduction is remote. In bacterial TrxR, a homologue of AhpF, one domain containing the pyridine nucleotide binding site and the redox-active disulfide center at distant locations twists back and forth, alternately delivering each site to the flavin; in the "pyridine nucleotide-near-flavin" conformation, the dithiol can interact with the disulfide bond of the Trx substrate for electron transfer (*25*). An alternative mechanism employed by the high-M_r form of TrxR expressed in higher organisms appears to involve no large domain movements; rather, a C-terminal "tail" provides an intermediary disulfide (or selenylsulfide) center to shuttle the electrons away from the flavin and proximal reduced disulfide center and over to the redox center of the Trx substrate. Interestingly, the C-terminal tail is provided by the other subunit of the dimer in this case. Biochemical and structural studies on a closely related protein which has a similar C-terminal dicysteine functionality, bacterial mercuric ion reductase, have firmly established the intersubunit interactions in that case (*26*, *27*). While the evidence for intersubunit disulfide center interactions in high-M_r TrxR is weaker, a recently reported heterodimer experiment with TrxR from *Plasmodium falciparum* does provide some insight (*24*). In this case, the heterodimer consisted of an inactive mutant containing disruptions in both disulfide centers (C88,535A) dimerized with wild type TrxR; this heterodimer was devoid of activity, purportedly due to the need for intersubunit interactions which could not occur with the mutant. The most exciting finding from this and our accompanying study (*7*) of AhpF has been that both large domain rotations (akin to those of bacterial TrxR) and interaction with an additional protein module bearing an extra disulfide redox center (like the C-terminal tail of high-M_r TrxR proteins) are used to accomplish protein disulfide reduction. Thus, multiple pathways accomplish similar redox chemistry in this highly interesting group of flavin-containing pyridine nucleotide: disulfide oxidoreductases (*25*).

In summary, the results obtained from the quantitation of the activities of two engineered heterodimers of AhpF have demonstrated that the transfer of electrons from the C-terminal to the N-terminal disulfide centers during catalysis is an intrasubunit process, in complete agreement with structural and modeling studies described in the accompanying report (*7*).

ACKNOWLEDGMENT

We thank Lois Laprade for constructing pAF[208-521]^{C345,348S}.

REFERENCES

1. Jacobson, F. S., Morgan, R. W., Christman, M. F., and Ames, B. N. (1989) *J. Biol. Chem. 264*, 1488−1496.
2. Poole, L. B., and Ellis, H. R. (1996) *Biochemistry 35*, 56−64.
3. Chae, H. Z., Robison, K., Poole, L. B., Church, G., Storz, G., and Rhee, S. G. (1994) *Proc. Natl. Acad. Sci. U.S.A. 91*, 7017−7021.
4. Tartaglia, L. A., Storz, G., Brodsky, M. H., Lai, A., and Ames, B. N. (1990) *J. Biol. Chem. 265*, 10535−10540.
5. Li Calzi, M., and Poole, L. B. (1997) *Biochemistry 36*, 13357−13364.
6. Poole, L. B., Godzik, A., Nayeem, A., and Schmitt, J. D. (2000) *Biochemistry 39*, 6602−6615.
7. Wood, Z. A., Poole, L. B., and Karplus, P. A. (2001) *Biochemistry 40*, 3900−3911.
8. Waksman, G., Krishna, T. S. R., Williams, C. H., Jr., and Kuriyan, J. (1994) *J. Mol. Biol. 236*, 800−816.
9. Poole, L. B., Reynolds, C. M., Wood, Z. A., Karplus, P. A., Ellis, H. R., and Li Calzi, M. (2000) *Eur. J. Biochem. 267*, 6126−6133.
10. Poole, L. B. (1996) *Biochemistry 35*, 65−75.
11. Poole, L. B. (1997) in *Flavins and Flavoproteins 1996* (Stevenson, K. J., Massey, V., and Williams, C. H., Jr., Eds.) pp 751−760, University of Calgary Press, Calgary, AB.
12. Guzman, L.-M., Belin, D., Carson, M. J., and Beckwith, J. (1995) *J. Bacteriol. 177*, 4121−4130.
13. Ausubel, F. M., Brent, R., Kingston, R. E., Moore, D. D., Seidman, J. G., Smith, J. A., and Struhl, K. (1992) *Short Protocols in Molecular Biology*, 2nd ed., John Wiley and Sons, New York.
14. Chung, C. T., Niemela, S. L., and Miller, R. H. (1989) *Proc. Natl. Acad. Sci. U.S.A. 86*, 2172−2175.
15. Bollag, D. M., and Edelstein, S. J. (1991) *Protein Methods*, Wiley-Liss, New York.
16. Johnson, M., Correia, J. J., Yphantis, D. A., and Halvorson, H. (1981) *Biophys. J. 36*, 575−588.
17. Laue, T. M., Shah, B. D., Ridgeway, T. M., and Pelletier, S. L. (1992) in *Analytical Ultracentrifugation in Biochemistry and Polymer Science* (Harding, S. E., Rowe, A. J., and Horton, J. C., Eds.) pp 90−125, The Royal Society of Chemistry, Cambridge, U.K.
18. Leatherbarrow, R. (1987) *ENZFITTER*, Biosoft, Cambridge, U.K.
19. Reynolds, C. M., and Poole, L. B. (2000) *Biochemistry 39*, 8859−8869.
20. Lennon, B. W., Williams, C. H., Jr., and Ludwig, M. L. (2000) *Science 289*, 1190−1194.
21. Carter, P., Bedouelle, H., and Winter, G. (1986) *Proc. Natl. Acad. Sci. U.S.A. 83*, 1189−1192.
22. Deonarain, M. P., Scrutton, N. S., and Perham, R. N. (1992) *Biochemistry 31*, 1491−1497.
23. Chan, J. M., Wu, W., Dean, D. R., and Seefeldt, L. C. (2000) *Biochemistry 39*, 7221−7228.
24. Krnajski, Z., Gilberger, T.-W., Walter, R. D., and Müller, S. (2000) *J. Biol. Chem. 275*, 40874−40878.
25. Williams, C. H., Jr., Arscott, L. D., Müller, S., Lennon, B. W., Ludwig, M. L., Wang, P.-F., Veine, D. M., Becker, K., and Schirmer, R. H. (2000) *Eur. J. Biochem. 267*, 6110−6117.
26. Distefano, M. D., Moore, M. J., and Walsh, C. T. (1990) *Biochemistry 29*, 2703−2713.
27. Schiering, N., Kabsch, W., Moore, M. J., Distefano, M. D., Walsh, C. T., and Pai, E. F. (1991) *Nature 352*, 168−172.

BI002766H